Asia-Pacific Journal of Science and Technology :Volume :30 .Issue :02 .Article ID :.APST-30-02-15. Research Article

APST

Asia-Pacific Journal of Science and Technology

https//:www.tci-thaijo.org/index.php/APST/index

Published by Research Department,
Khon Kaen University, Thailand

Thickness optimization of a triple-layered microwave absorber combining magnetic and dielectric particles

Affandi Faisal Kurniawan [1,2*], Mohammad Syaiful Anwar [2], Khoirotun Nadiyyah [3], I Gusti Ngurah Nitya Santhiarsa [4], Mashuri [2], Triwikantoro [2] and Darminto[2*]

[1] Physics Education Study Program, Faculty of Mathematics, Natural Science, Information Technology Education, Universitas PGRI Semarang, Semarang 50232, Indonesia
[2] Advanced Materials Research Group, Department of Physics, Faculty of Science and Analytics Data, Institut Teknologi Sepuluh Nopember, Sukolilo, Surabaya 60111, Indonesia
[3] Physics Education Study Program, Faculty of Education and Teacher Training, Universitas Terbuka, Tangerang Selatan 15437, Indonesia.
[4] Mechanical Engineering Study Program, Faculty of Engineering, University of Udayana, Bukit Jimbaran, Bali 80361, Indonesia.
[*]Corresponding author: affandifaisal@upgris.ac.id

Received 29 April 2023
Revised 27 September 2024
Accepted 1 October 2024

Abstract

The objective of this research is to optimize the thickness of a triple-layer microwave absorber using a genetic algorithm (GA). The materials employed in this study consist of a combination of magnetic and dielectric materials, along treated dielectric material, to create a triple-layer absorber. S-parameters (S_{11} and S_{21}) were obtained from measurements of these materials with a thickness of 2 mm using a Vector Network Analyzer (VNA). Input parameters, including relative complex permeability and relative complex permittivity, were derived by converting the S-parameters using a conversion program based on the Nicolson-Ross-Weir (NRW) method. The thickness of each sample was optimized using GA to achieve a high reflection loss value ($RL_{\min}$) by entering the relative complex permeability and relative complex permittivity values. The results indicate that the optimization of the thickness of the reflection loss equation for the triple-layer absorber from six triple-layer absorber results in high RL_{min} (-61.76 dB) at optimum thickness of d_1= 2.17 mm, d_2 = 1.6 mm, and d_3 = 3.76 mm at a frequency of 10.76 GHz, with a bandwidth of 0.58 GHz. Optimizing the thickness and the number of layers is crucial in the design of triple-layer radar absorbing materials (RAM) and can produce high values of RL_{min}.

Keywords: Genetic algorithm, High absorption, Thickness optimization, Triple-layer absorber

1. Introduction

In both military and civilian applications, multilayer microwave absorbers play a vital role due to their ability to minimize reflection and absorb electromagnetic radiation waves [1,2]. The absorption of radiation occurs through two mechanisms: the first mechanism reduces reflection by providing a gradually changing impedance matching layer, while the second mechanism enhances absorption through the use of high-loss materials in the back layer [3]. In a multilayer microwave absorber, a material with a high impedance is placed in the front layer to minimize reflection between the absorber and air [3]. Microwave absorbers with multilayer structures exhibit a wider absorption bandwidth and lower reflection loss compared to single-layer structures in the gigahertz frequency range [4,5].

The design of a microwave absorber depends on several criteria, including the number of layers, fill weight percentage, thickness, frequency, angle of incidence, permittivity, permeability, and polarization [6,7]. Various researchers have developed microwave absorber optimization techniques based on these parameters using different evolutionary algorithms, such as particle swarm optimization (PSO) [8,9], genetic algorithms (GA) [10], winning particle optimization (WPO) [11], and self-adaptive differential evolutionary algorithms (SADEA) [12].

Among these evolutionary algorithms, GA is particularly effective for designing multilayer microwave absorbers [6]. GA possesses powerful and efficient guidance features [10]. Some advantages of GA include a broader solution space, the ability to navigate complex fitness landscapes, ease of finding global optima, suitability

Several researchers have explored the development of nanostructure-based tunable perfect absorbers, both experimentally and theoretically. For instance, experimental studies have investigated ultra-narrow perfect absorbers through cascaded two-cavity structures [14]. Additionally, theoretical investigations have focused on perfect absorbers based on metal line structures in the visible and near-infrared regions [15]. Other research has designed and studied wide-angle double-band plasmonic absorbers composed of a split metal-dielectric-metal square rings and square arrays [16].

Furthermore, several studies have addressed perfect absorbers, including theoretical investigations of polarization-independent perfect absorbers through three-layer lattice structures [17]. Other theoretical research has examined tunable perfect absorbers based on split metal-dielectric-metal square rings and square arrangements [16]. In addition, Bruck et al. [18] designed an integrated coherent plasmonic absorber using a plasmonic nanoantenna array on silicon in an insulator waveguide.

Research on tunable absorption using graphene has also gained attention. For example, in 2016, studies focused on the tunable light absorption of graphene-coupled multilayer photonic structures [19]. The following year, numerical studies investigated complete absorption in monolayer molybdenum disulfide (MoS_2) [20]. Additionally, research has designed ultralight and highly compressible graphene foam (GF, 0.14 mg/cm^3) a wide bandwidth of 60.5 GHz, covering 93.8% of the total bandwidth [21].

This paper presents a microwave absorber designed based on thickness optimization using GA and an increased number of layers (triple-layer absorber) to achieve excellent absorption properties. The materials used in this study, sourced from natural materials, include a combination of magnetic material (Tanah Laut iron stone, South Kalimantan, Indonesia) and dielectric materials (pure old coconut shell and treated old coconut shell). The design is also based on the complex relative permittivity and complex permeability values, utilizing a computer program based on the Nicolson-Ross-Weir (NRW) method, material selection for each layer in the triple layer absorber, and thickness selection for each layer based on thickness optimization using GA. The novelty of this work lies in the optimization of the Radar Absorber Material (RAM) triple-layer sample thickness using a genetic algorithm (AG), which predicts the appropriate thickness so that the high RL_{min} can be obtained.

2. Materials and methods

2.1 Sample Preparation and Characterization

Fe_3O_4 powder (sample M2) was obtained from rocks in Tanah Laut (South Kalimantan). To obtain coarse powder, the stone was crushed using a mortar and pestle. The coarse powder was then sieved through a 200 mesh to obtain fine powder with uniformly sized particles, maximizing surface area for even distribution. After sample formation, characterization was performed using X-ray diffractometry (XRD) for phase analysis and reflection loss measurements using a Vector Network Analyzer (VNA). The results of this characterization serve as input variables for thickness optimization using GA.

To obtain maximum rGO powder (sample M1), old coconut shells were dried in the sun for one day and then burned to form black charcoal. The ingredients were subsequently ground a mortar and sifted through a 200 mesh to produce charcoal powder. This powder was placed in a container for carbonization, with the heating process conducted in a furnace for 5 hours at a temperature of 400 °C [22].

The chemical exfoliation process involved mixing 100 mL of 1M HCl solution the powder that had undergone the heating process. The mixture was stirred using a magnetic stirrer at 70 °C for 20 hours, with a rotation speed of 350 rpm [22]. In this study, the mole ratio between the 1M HCl solution and rGO powder was 1:10 (sample M3).

2.2 Triple-Layer Design of Microwave Absorber Material

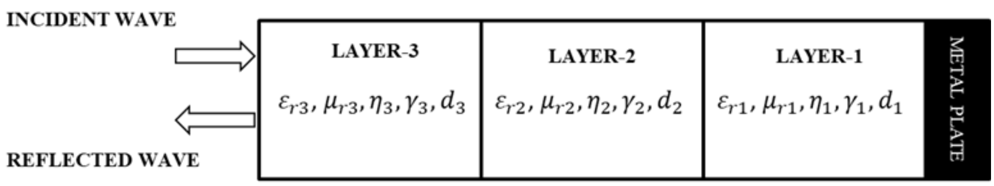

Figure 1 A schematic diagram of a triple-layer absorber

A three-layer graded dielectric absorber supported by a conductor can be designed as shown in Figure 1. The principle of the three-layer microwave absorption is similar to that of a double-layer dielectric absorber. The input impedance at the absorber's front layer is calculated by substituting the equations for the input impedances Z_2 and Z_1 of the metal-supported inner layer into the general Equation 1. Considering the conductivity of the individual layers as zero, the input impedance for the reflection loss equation for the triple-layer absorber can be derived accordingly [23]:

$$Z_{in} = \eta_i \frac{Z_{i-1} + \eta_1 \tanh\gamma_1 d_1}{\eta_i + Z_{i-1}\tanh\gamma_1 d_1} \tag{1}$$

$$Z_3 = Z_{in} = \eta_3 \frac{Z_2 + \eta_3 \, tanh\gamma_3 d_3}{\eta_3 + Z_2 tanh\gamma_3 d_3} \tag{2}$$

$$\eta_3 = \eta_0 \sqrt{\mu_{r3}/\varepsilon_{r3}} \tag{3}$$

$$\gamma_3 = j\left(\frac{2\pi f}{c}\right)\sqrt{\mu_{r3}\varepsilon_{r3}} \tag{4}$$

Thus, the reflection loss (dB) of the triple-layer absorber can be derived accordingly [23]:

$$RL_C = 20\log\left|\frac{\frac{a}{b}\eta_0\eta_3}{\eta_3\frac{a}{b} + \eta_0}\right| \tag{5}$$

$$a = \eta_2 \frac{\eta_1 tanh\gamma_1 d_1 + \eta_2 tanh\gamma_2 d_2}{\eta_2 + \eta_1 \tanh(\gamma_1 d_1)\tan\mathrm{h}(\gamma_2 d_2)} + \eta_3 tanh\gamma_3 d_3$$

$$b = \eta_3 + \eta_2 \frac{\eta_1 tanh\gamma_1 d_1 + \eta_2 tanh\gamma_2 d_2}{\eta_2 + \eta_1 \tan\mathrm{h}(\gamma_1 d_1)\tan\mathrm{h}(\gamma_2 d_2)} tanh\gamma_3 d_3$$

In accordance the recommendations of optimization experts GA, Grafenstette and De Jong, the population size (PopSize), crossover probability (Pc), and mutation probability (Pm) are the parameters used in optimization. In addition to optimization parameters, the process also requires input variables, output variables, fitness functions, and constrained optimization. The conditions to be optimized are referred to as input variables, including the number of generations (makgen), fitness threshold (fthreshold), frequency, speed of light, permeability, and permittivity. The permeability values ($\mu_r = \mu' - j\mu''$) And permittivity ($\varepsilon_r = \varepsilon' - j\varepsilon''$) were obtained from single-layer absorb VNA data, specifically S_{11} (reflection coefficient) and S_{21} (transmission coefficient), which were converted using the Nicolson-Ross-Weir (NRW) method with software developed in MATLAB. The output variable sought in this research is the thickness of the material for the triple-layer absorber. The GA method optimization requires defining the mathematical model into the fitness function. The triple-layer absorber from Eq. 1 to Eq. 5 serves as the mathematical model to be optimized. Constrained optimization is necessary because the dimensions of reflection loss have predetermined limits for incorporating these variables into the fitness function.

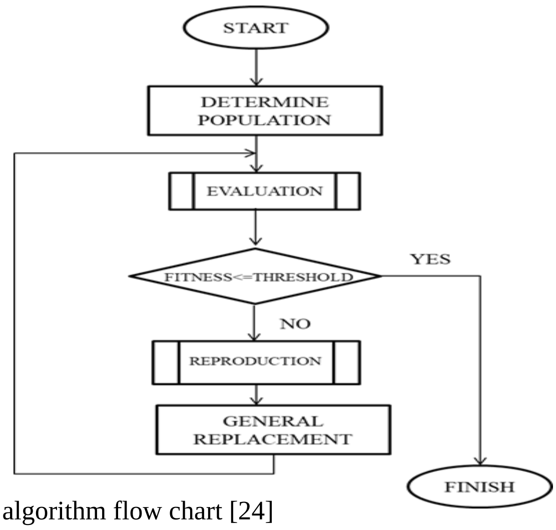

Figure 2 illustrates the genetic algorithm flow chart [24]

Optimization employs standard genetic algorithm techniques (Figure 2). The steps are as follows: first, determine the population; second, evaluate using binary coding and linear fitness rankings; third, reproduce through elitism; fourth, select using the roulette wheel; fifth, perform crossover and mutation; and finally, conduct general substitution. After completing the optimization process, the next step is to display the simulation and optimization results. The simulation results of the reflection loss equation for the triple-layer absorber thickness optimization using the GA method, which show the fitness value throughout the optimization process, are necessary to determine the optimization route and the reflection loss results achieved. The optimization results are reflected in the thickness of the material in the triple-layer absorber. Additionally, a graph simulation illustrating the relationship between frequency and the reflection loss value based on the thickness optimization results is presented.

2.3 Composite Preparation and Double-Layer Reflection Loss Characterization

Samples M1, M2, and M3 are the absorber materials selected for this study. The preparation of these samples has been discussed previously [24]. Six different combinations of the triple-layer material absorber arrangement are summarized in Table 2.

Table 2 Combined triple-layer absorber design.

Air-absorber interface layer	Sample combination I-II-III layers
M1-Interface	M2-M3-M1
	M3-M2-M1
M2-Interface	M1-M3-M2
	M3-M1-M2
M3-Interface	M2-M1-M3
	M1-M2-M3

3. Results and Discussion

3.1 Dielectric Properties

The dielectric parameters of M1, M2, and M3 composites, including real relative permeability (μ'), imaginary permeability $\left(\mu''\right)$, real permittivity (ε'), and imaginary permittivity (ε'') shown in Figure 3 (a) and Figure 3 (b). Real permittivity and real permeability represent the amount of electric and magnetic energy stored, while the imaginary components of permittivity and permeability represent the loss and dissipation of electric and magnetic energy [25]. The dielectric parameters were obtained from the conversion of S-parameter (S_{11} and S_{21}) single-layer absorbers M1, M2, and M3 VNA data using a program developed with the NRW method in MATLAB.

Figure 3 (A) shows that ε' and ε'' have two peaks in each sample. The peaks occur at approximately 8.3–9.5 GHz and 10.50–11.5 GHz. At both peaks, the values of $\varepsilon'$and $\varepsilon''$from smallest to largest as follows: samples M1, M3, and M2, respectively. The largest and smallest values of ε' and ε'' are sample M2 (pure magnetic material) and sample M1 (pure non-magnetic material), respectively. Meanwhile, μ' dan μ'' in Figure 3 (B), the real and imaginary permittivity also exhibit two peaks in each sample. The frequency range for the first peak is approximately 9.3–10.6 GHz, while the second peak occurs at approximately 11.5–12 GHz. The magnitudes of μ' from large to smallest are M1 (pure non-magnetic material), M2 (pure magnetic material), and M3 (treated non-magnetic material), respectively. For the magnitude of μ'' on the magnitudes of imaginary permittivity are M2 (pure magnetic material), M1 (pure non-magnetic material), and M3 (treated non-magnetic material), respectively. At the second peak, the magnitudes of magnitude μ'' respectively from largest to smallest are M1 (pure non-magnetic material), M2 (pure magnetic material), and M3 (treated non-magnetic material). Microwave absorbers can be classified as single-layer or multi-layer structures. Single-layer structures can simultaneously exhibit impedance matching and attenuation functions, while in multilayer absorbers, impedance matching is controlled by one material and attenuation is governed by another material [27].

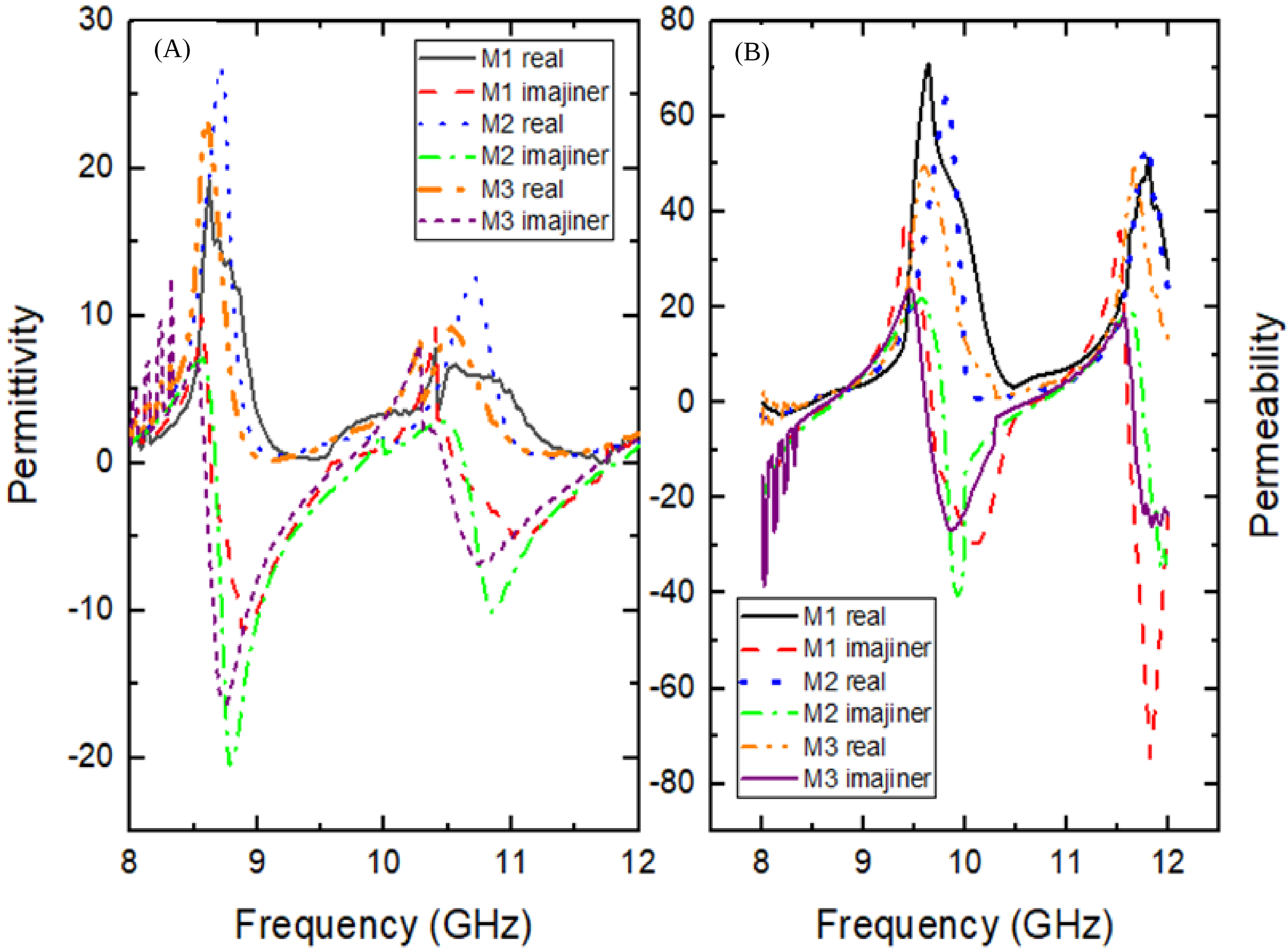

Figure 3 (A) Real and imaginary permittivity for all samples, (B) Real permeability and imaginary permeability for all samples.

3.2 Reflection Loss of Triple-Layer Design

The multi-layer absorber design, in this study the reflection loss equation for the triple-layer absorber, aims to optimize the composition and thickness of the layers to achieve an optimal reflection loss value (RL_{min} <-20 dB). To accomplish this, two fundamental conditions must be meet the following requirements [5,28]: (a) the impedance-matching characteristic, which ensures that the incident wave enters the absorber as effectively as possible, and (b) the attenuation characteristics, which require that nearly all electromagnetic waves entering the material are attenuated and absorbed in the material's infinite thickness. The multi-layer absorber design, enhanced by the optimization of the triple-layer absorber thickness using GA, fulfills these two fundamental conditions. Figure 1 provides a simplified diagram of a conductor-backed triple-layer absorber with intrinsic parameters ε_{r1}, $\mu_{r1}, \eta_1, \gamma_1, d_1$ for layer-1 adjacent to the metal plate, layer-2 with intrinsic parameters ε_{r2}, $\mu_{r2}, \eta_2, \gamma_2, d_2$ as sandwiched layer, and intrinsic parameters ε_{r3}, $\mu_{r3}, \eta_3, \gamma_3, d_3$ for front-facing layer-3 facing the vacuum.

The reflection loss equation for the reflection loss equation for the triple-layer absorber (Equation 5) indicates that the reflection loss value depends on the complex permittivity and frequency-dependent complex permeability (ε_{r1}, ε_{r2}, ε_{r3} , μ_{r1}, μ_{r2}, μ_{r3}) and the thicknesses of each layer d_1, d_2, and d_3. The minimum reflection loss value (RL_{min}) was achieved by optimizing the intrinsic effective properties of the three layers and their respective thicknesses. Six combinations of triple-layer absorber designs are presented in Table 3.

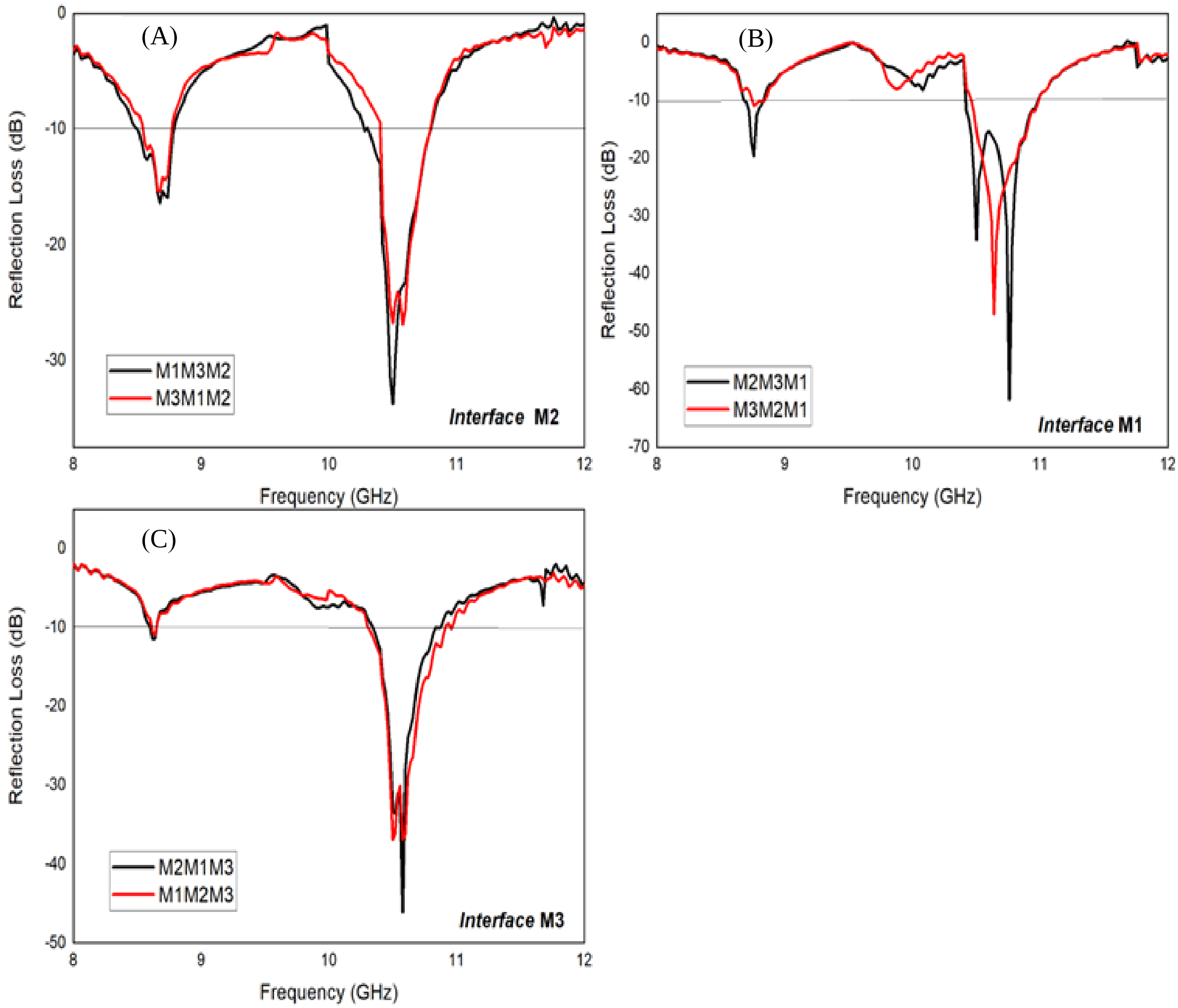

Figure 4 Reflection Loss Triple-layer Absorber, (A) Interface M2, (B) Interface M1, and (C) Interface M3.

The results of the triple-layer microwave absorber thickness optimization using GA for interfaces M1, M2, and M3, as discussed previously in Section 2. The reflection loss equation for the triple-layer absorber design achieves a value of $-26.91\ dB \leq RL_{min} \leq\ -61.76\ dB$. In designing the triple-layer absorber, the frequency position can be adjusted as desired. Figures 4 (A), (B), and (C) show the reflection loss values as a function of frequency for the M2 triple-layer absorber interface design, specifically M1-M3-M2 and M3-M1-M2 (Figure 4 (A)), the M1 absorber interface layer, namely M2-M3-M1 and M3-M2-M1 (Figure 4 (B)), and the M3 triple-layer absorber interface, specifically M2-M1-M3 and M1-M2-M3 (Figure 4 (C)) thickness optimization results is presented. The minimum reflection loss (RL_{min}) based on the thickness optimization results using GA, frequency, bandwidth, and thickness of each layer optimized using GA are tabulated in Table 3.

Figure 4 and Table 3 indicate that all triple-layer absorber design combinations show a reflection loss value of RL_{min} < -20 dB. The value of RL_{min} < -20 dB and bandwidth is from the M2-M3-M1 (interface M1) sample design, which achieves -61.76 dB at a frequency of 10.76 GHz, a bandwidth of 0.58 GHz and a total thickness of 7.53 mm. Meanwhile, the reflection loss equation for the triple-layer absorber design combination M3-M1-M2 demonstrates the smallest RL_{min} and bandwidth values, measuring -26.91 dB and 0.4 GHz, respectively. In this research, the materials utilized are M1, M2, and M3. The combination of materials in the triple-layer absorber design significantly influences the value of RL_{min}. This aligns with findings from previous studies [28], which indicate that the arrangement of materials in both double-layer and triple-layer absorber designs affects the value of. RL_{min} and bandwidth. Additionally, increasing the number of layers can enhance the value of RL_{min}. These results corroborate prior research [2,28].

Table 3 The result of thickness optimization and the optimization result of the RL_{min} GA for the triple-layer absorber.

No	*Triple-Layer Absorber*	d1 (mm)	d2 (mm)	d3 (mm)	Total thickness (mm)	RL_{min} (dB)	Frequency (GHz)	Bandwidth (GHz)
1	M1-M3-M2	2.24	0.75	1.05	4.04	-33.73	10.5	0.5
2	M3-M1-M2	0.5	2.45	1.06	4.01	-26.91	10.58	0.4
3	M2-M3-M1	2.17	1.6	3.76	7.53	-61.76	10.76	0.58
4	M3-M2-M1	0.54	0.9	3.93	5.37	-47.03	10.64	0.54
5	M2-M1-M3	2.24	0.5	1.54	4.28	-46.08	10.58	0.5
6	M1-M2-M3	1.23	1.35	1.62	4.2	-36.91	10.5	0.62

4. Conclusion

The triple-layer radar absorber material (RAM) thickness optimization program developed in MATLAB has been successfully implemented. This program plays a crucial role in designing triple-layer RAM to produce high RL_{min} values. The highest absorption observed in this study is the combination of the M2 sample, M3 sample, and M1 sample a total thickness of 7.53 mm. The value of RL_{min}, thickness of each layer, frequency, and bandwidth are -61.76 dB, at optimum thickness d_1= 2.17 mm, d_2 = 1.6 mm, and d_3 = 3.76 mm, at a frequency of 10.76 GHz with bandwidth of 0.58 GHz. The six samples used in the triple-layer RAM thickness optimization in this research can produce a value of RL_{min} < -25 dB, which is superior to those of single-layer and double-layer RAM. The six samples of triple-layer RAM investigated in this study demonstrate effective microwave absorption in X-band frequencies. The optimization of RAM thickness using GA and the increase in the number of layers contribute to more effective and efficient experiments, enhancing the value of RL_{min}.

5. References

[1] Dib NI, Asi M, Sabbah A. On The Optimal Design of Multilayer Microwave Absorbers. Prog Electromagn Res. 2010:171–185.

[2] Abdullah H, Zanal A, Ahya Ilmudin MH, Taib MN, Sharif JMd, Nizam Malek MK, Baharudin R., Mohamed Noordin IR, Razali AR. Characteristic Evaluation of Multiple Layers Microwave Absorber Coated Biomass Composite. Appl Mech Mater. 2016: 88–92.

[3] Salleh MKM, Yahya M, Awang Z, Muhamad WNW, Mozi AM, Yaacob N. Binomial multi-layer coconut shell-based rubber microwave absorber design. IEEE International RF and Microwave Conference (RFM) (Seremban, Negeri Sembilan, Malaysia: IEEE). 2011:187–190.

[4] Cao M, Zhu J, Yuan J, Zhang T, Peng Z, Gao Z, et al. Computation design and performance prediction towards a multi-layer microwave absorber. Mater Des. 2002:557–564.

[5] Zhang X, Sun W. Three-layer microwave absorber using cement-based composites. Mag Concr Res. 2011:157–162.

[6] Santhosi BVSRN, Ramji K, Rao NBR. Optimization of double layered graphene-based microwave absorber in X—band using Pareto genetic algorithm. Mater Res Express. 2019: 105610.

[7] Mouna H, Mekaladevi V, Nirmala Devi M. Design of Microwave Absorbers using Improvised Particle Swarm Optimization Algorithm. J Microw Optoelectron Electromagn Appl. 2018:188–200.

[8] Gies D, Rahmat-Samii Y. Particle swarm optimization for reconfigurable phase-differentiated array design. Microw. Opt Technol Lett. 2003: 168–175.

[9] Yu-Bo T, Yue D, Zhi-Bin X, Sha S, Tao P. Frequency characteristics of electromagnetic bandgap structure bow-tie cells and its optimal design based on particle swarm optimization. IEEJ Trans Electr Electron Eng. 2013: 63–68.

[10] Chen X, Liu XX, Wang XJ, Liu Y. Optimized Design for Multi-Layer Absorbing Materials Based on Genetic Algorithm. Adv Mater Res. 2013: 324–328.

[11] Micheli D., Pastore R, Marchetti M. Modeling of radar absorbing materials using winning particle optimization applied on electricallyconductive nanostructured composite material. Int J Mat Sci. 2012:31–38.

[12] Goudos SK. Design of microwave broadband absorbers using a self-adaptive differential evolution algorithm: absorber design using self-adaptive dE. Int J RF Microw Comput Aided Eng. 2009: 364–372.

[13] Sivanandam SN, Deepa SN. Introduction to Genetic Algorithms. Berlin Heidelberg: Springer-Verlag; 2008.

[14] Zhao D, Meng L, Gong H, Chen X, Chen Y, Yan M, et al. Ultra narrow band light dissipation by a stack of lamellar silver and alumina. Appl Phys Lett. 2014; 104: 221107.

[15] Shu SW, Li YY. Metallic rugate structures for near perfect absorbers in visible and near infrared regions. Opt Lett. 2012; 7(17):3495–3497.

[16] Lee HM, Wu JC. A wide-angle dual band infrared perfect absorber based on metal-dielectric-metal split square ring and square array. J Phys D Appl. 2012; 45(20): 205101.

[17] Lin CH, Chern RL, Lin HY. Polarization independent broadband nearly perfect absorbers in the visible regime. Opt Express. 2011; 19(2): 415–424.

[18] Bruck R, Muskens OL. Plasmonic nanoantennas as integrated coherent perfect absorbers on SOI waveguides for modulators and all-optical switches. Opt Express. 2013; 21(23):27662–27671.

[19] Lu H, Gan XT, Jia BH, Mao D, Zhao JL. Tunable high-efficiency light absorption of monolayer graphene via Tamm plasmon polaritons. Opt Lett.: 2016; 41(20): 4743–4746.

[20] Lu H, Gan XT, Mao D, Fan YC, Yang DX, Zhao JL. Nearly perfect absorption of light in monolayer molybdenum disulfide supported by multilayer structures. Opt Express. 2017; 25(18): 21630–21636.

[21] Zhang Y, Huang Y, Zhang TF, Chang HC, Xiao PS, Chen HH, et al. Broadband and tunable high-performance microwave absorption of an ultralight and highly compressible graphene foam. Adv Mater. 2015; 27(12): 2049–2053.

[22] Kurniawan AF, Anwar MS, Nadiyyah K, Mashuri M, Triwikantoro T, Darminto D. Mechanical Exfoliation of Reduced Graphene Oxide from Old Coconut Shell as Radar Absorber in X-Band. Mater Sci Forum. 2019: 25–29.

[23] Gogoi JP. Expanded graphite novolac phenolic resin based electromagnetic interference EMI shielding material over the X band: synthesis characterization analysis and design optimization [Dissertation]. Assam: Tezpur University; 2012.

[24] Kurniawan AF, Anwar MS, Nadiyyah K, Mashuri M, Triwikantoro T, Darminto D. Thickness optimization of a double-layered microwave absorber combining magnetic and dielectric particles. Mater Res Express. 2021; 8: 065001.

[25] Ni Q-Q, Melvin GJH, Natsuki T. Double-layer electromagnetic wave absorber based on barium titanate/carbon nanotube nanocomposites. Ceram Int. 2015: 9885–9892.

[26] Duggal S, Aul GD. review on effect of electric permittivity and magnetic permeability over microwave absorbing materials at low frequencies. Int J Eng Adv Technol. 2014: 12–19.

[27] Zhang B, Feng Y, Xiong J, Yang Y, Huaixian L. Microwave-absorbing properties of de-aggregated flake-shaped carbonyl-iron particle composites at 2-18 GHz. IEEE Trans Magn. 2006: 1778–1781.

[28] Micheli D, Pastore R, Apollo C, Marchetti M, Gradoni G, Primiani VM, et al. Broadband electromagnetic absorbers using carbon nanostructure-based composites. IEEE Trans Microw. Theory Tech. 2011: 2633–2646.